


# High performance planar microcavity organic semiconductor lasers based on thermally evaporated top distributed Bragg reflector

Cite as: Appl. Phys. Lett. **117**, 153301 (2020); <https://doi.org/10.1063/5.0016052>

Submitted: 02 June 2020 . Accepted: 30 August 2020 . Published Online: 13 October 2020

 Yongsheng Hu,  Fatima Bencheikh,  Sébastien Chénais,  Sébastien Forget,  Xingyuan Liu, and  Chihaya Adachi

## COLLECTIONS

 This paper was selected as Featured



View Online



Export Citation



CrossMark

## ARTICLES YOU MAY BE INTERESTED IN

Intramolecular-rotation driven triplet-to-singlet upconversion and fluctuation induced fluorescence activation in linearly connected donor-acceptor molecules

The Journal of Chemical Physics **153**, 204702 (2020); <https://doi.org/10.1063/5.0029608>

Thickness-dependent electronic transport induced by in situ transformation of point defects in MBE-grown Bi<sub>2</sub>Te<sub>3</sub> thin films

Applied Physics Letters **117**, 153902 (2020); <https://doi.org/10.1063/5.0025828>

A non-invasive gating method for probing 2D electron systems on pristine, intrinsic H-Si(111) surfaces

Applied Physics Letters **117**, 151603 (2020); <https://doi.org/10.1063/5.0024842>



**HIDEN**  
ANALYTICAL

## Instruments for Advanced Science

- Knowledge,
- Experience,
- Expertise

[Click to view our product catalogue](#)

Contact Hiden Analytical for further details:

 [www.HidenAnalytical.com](http://www.HidenAnalytical.com)  
 [info@hiden.co.uk](mailto:info@hiden.co.uk)

### Gas Analysis

- dynamic measurement of reaction gas streams
- catalysis and thermal analysis
- molecular beam studies
- dissolved species probes
- fermentation, environmental and ecological studies

### Surface Science

- UHVTPD
- SIMS
- end point detection in ion beam etch
- elemental imaging - surface mapping

### Plasma Diagnostics

- plasma source characterization
- etch and deposition process reaction kinetic studies
- analysis of neutral and radical species

### Vacuum Analysis

- partial pressure measurement and control of process gases
- reactive sputter process control
- vacuum diagnostics
- vacuum coating process monitoring

# High performance planar microcavity organic semiconductor lasers based on thermally evaporated top distributed Bragg reflector

Cite as: Appl. Phys. Lett. **117**, 153301 (2020); doi: [10.1063/5.0016052](https://doi.org/10.1063/5.0016052)

Submitted: 2 June 2020 · Accepted: 30 August 2020 ·

Published Online: 13 October 2020



View Online



Export Citation



CrossMark

Yongsheng Hu,<sup>1</sup>  Fatima Bencheikh,<sup>2,3,a)</sup>  Sébastien Chénais,<sup>3,4</sup>  Sébastien Forget,<sup>3,4</sup>  Xingyuan Liu,<sup>1,a)</sup>  and Chihaya Adachi<sup>2,3,5,a)</sup> 

## AFFILIATIONS

<sup>1</sup>State Key Laboratory of Luminescence and Applications, Changchun Institute of Optics, Fine Mechanics and Physics, Chinese Academy of Sciences, Changchun 130033, China

<sup>2</sup>Center for Organic Photonics and Electronics Research (OPERA), Kyushu University, 744 Motooka, Nishi, Fukuoka 819-0395, Japan

<sup>3</sup>Japan Science and Technology Agency (JST), ERATO, Adachi Molecular Exciton Engineering Project, 744 Motooka, Nishi, Fukuoka 819-0395, Japan

<sup>4</sup>Laboratoire de Physique des Lasers (LPL), Université Sorbonne Paris Nord, CNRS, UMR 7538, Villetaneuse F-93430, France

<sup>5</sup>International Institute for Carbon-Neutral Energy Research (WPI-I2CNER), Kyushu University, 744 Motooka, Nishi, Fukuoka 819-0395, Japan

<sup>a)</sup>Authors to whom correspondence should be addressed: [bencheikh.fatima.482@m.kyushu-u.ac.jp](mailto:bencheikh.fatima.482@m.kyushu-u.ac.jp); [liuxy@ciomp.ac.cn](mailto:liuxy@ciomp.ac.cn); and [adachi@cstf.kyushu-u.ac.jp](mailto:adachi@cstf.kyushu-u.ac.jp)

## ABSTRACT

High performance organic semiconductor lasers (OSLs), especially those under current injection, have been sought for decades due to their potentially great applications in fields such as spectroscopy, displays, medical devices, and optical interconnection. The design and fabrication of high-quality resonators is a prerequisite for high performance OSLs. In the case of planar microcavities, the fabrication process of top distributed Bragg reflectors (DBRs) usually requires electron beam evaporation or manual lamination on top of organic thin-film layers, which can lead to issues including degradation of the organic materials, large-scale non-uniformity, and difficulties for current injection. Here, we report a non-destructive way of fabricating a top DBR by thermal evaporation. The top DBR based on thermally evaporated alternative  $\text{TeO}_x/\text{LiF}$  stacks shows low morphological roughness, high process tolerance, and high reflectivity. Moreover, the deposition process causes negligible damage to the organic thin-film layers underneath. With the combination of a conventional e-beam evaporated bottom DBR, a high performance planar microcavity OSL with a low threshold of  $1.7 \mu\text{J cm}^{-2}$ , an emission linewidth of 0.24 nm, and an angular divergence of  $<3^\circ$  has been achieved under nitrogen laser pumping. Similar performance, with a high Gaussian beam quality comparable with that of an ideal diffraction-limited beam, was also obtained under diode pumping, showing the potential of this technique for building compact and cost-effective organic lasers with good beam quality. Our result will open a promising route for future high performance microcavity optoelectronic devices, especially for laser devices under current injection.

Published under license by AIP Publishing. <https://doi.org/10.1063/5.0016052>

Organic semiconductor lasers (OSLs) have gained wide attention as promising low-cost, color-tunable, and flexible laser sources in the past few decades.<sup>1–3</sup> The design and fabrication of high quality resonators is a prerequisite for high performance OSLs. Distributed feedback (DFB) gratings<sup>4–9</sup> and planar microcavities<sup>10–15</sup> are the two most widely adopted resonators for OSLs. Recently, an indication of lasing behavior from a current injection OSL diode (OSLD) has been

reported with a thin-film device architecture incorporating a DFB grating.<sup>16</sup> DFB OSLs have many advantages such as large gain volume, low threshold, and easy fabrication. However, they also have several drawbacks such as poor beam quality (e.g., a fan shaped beam) and large fluctuations in organic thin film layers as a result of the periodic grating structures.<sup>6,16</sup> In contrast, planar microcavities or organic vertical cavity surface-emitting lasers (OVCSELs)<sup>1</sup> consist of two closely

parallel highly reflective distributed Bragg reflectors (DBRs) formed by stacking alternative dielectrics. In spite of the short cavity and low round trip gain, the OVCSELs exhibit good output beam quality, ultra-compactness, and ease for integration.

Generally, DBR mirrors are fabricated by sputtering, plasma-enhanced chemical vapor deposition (PECVD), or high temperature e-beam evaporation.<sup>11,17–19</sup> These methods are adequate to fabricate DBRs with very high optical quality on top of inorganic crystals or glasses. However, if DBR mirrors are fabricated on top of soft materials such as organic semiconductors, colloidal quantum dots, and perovskites, significant damage can be caused, resulting in the deterioration of the device performances.<sup>2,19,20</sup> Therefore, most OVCSELs are formed by either thermally evaporating a metal layer as the top mirror or manually laminating two prefabricated DBRs.<sup>10,21–23</sup> Nevertheless, the former is not suitable for a high quality microcavity due to its relatively low reflectance and large absorption loss from the metal layer, while for the latter, the issues such as device uniformity, large-scale integration, and compatibility with current-injection type lasers are not easy to be addressed.

Alternatively, methods such as thermal evaporation, solution process, and low temperature e-beam evaporation have been developed.<sup>20,24–28</sup> DBRs fabricated by these methods show both high reflectivity and good uniformity. More attractively, these methods are believed to be less destructive to organic thin-film layers. However, so far, there are only a few works that demonstrate organic lasing based on these methods and the lasing thresholds of these devices are still very high.<sup>20,27,28</sup>

In this work, we demonstrate that a high quality top DBR mirror can be obtained by using thermal evaporation with the all fabrication process compatibility with organic gain layers. OVCSELs with ultra-low threshold, narrow emission, and good directionality have been achieved. Not only these features were obtained under nitrogen laser pumping but also they were conserved under diode-pumping, which allowed a much more compact/cost-effective device architecture.

The schematic diagram of the OVCSEL is shown in Fig. 1(a). A stack of 15.5 pairs of  $\text{TiO}_2/\text{SiO}_2$  was used as the bottom DBR, which

was fabricated by conventional high temperature e-beam evaporation with an assisted end-Hall ion source.<sup>29</sup> For the gain layer ( $\sim 110$  nm), we chose 4,4'-bis[(N-carbazole)styryl]biphenyl [BSBCz, Fig. 1(b)], as this material has shown ultra-low thresholds, quasi-CW lasing, and recently the first indication of electrical pumping in DFB resonators.<sup>6,16</sup> Here, BSBCz was used as a dopant (6 wt.%) in a 4,4'-bis(N-carbazolyl)-1,1'-biphenyl [CBP, Fig. 1(b)] host. As for the top DBR, we chose  $\text{TeO}_x/\text{LiF}$  with a layer thickness of  $\lambda_c/4n$  ( $\lambda_c$  is the central wavelength and  $n$  is the refractive index) due to the high refractive index difference and negligible absorption in the visible region (Fig. S1). Also, the evaporation temperatures for  $\text{TeO}_x$  and LiF are appreciably low of 733 °C and 848 °C, respectively, rendering them suitable for thermal evaporation.<sup>24,26</sup>

We first examined the morphology of the top DBR. Figure S2 shows that the  $\text{TeO}_x$  film has a very smooth morphology with a root mean square (RMS) roughness of only 0.51 nm, while that for the LiF film shows appreciably higher roughness with the RMS of 2.69 nm. The surface of the top DBR [Fig. 1(c)] has a reduced RMS roughness (1.26 nm) compared to that of the LiF film, which can be attributed to the filling effect by the smaller  $\text{TeO}_x$  particles since both  $\text{TeO}_x$  and LiF have a particulate morphology. It is noticed that the base pressure of the chamber has a negligible impact on the film morphology (Fig. S3). This indicates a high tolerance for the thermal evaporation process in contrast to other methods such as PECVD and e-beam evaporation, which usually require accurate control of the atmosphere and pressure. The low morphology roughness is important for reducing the light scattering and diffraction loss, thus guaranteeing a high-quality resonator.<sup>30</sup> The roughness of the as-fabricated top DBR is comparable to that in the literature.<sup>17</sup>

Next, we investigated the influence of the top DBR evaporation process on the gain material. A  $\text{TeO}_x$  (60 nm) layer was deposited onto a BSBCz:CBP layer (100 nm), and the photoluminescence quantum yield (PLQY) was examined. As shown in Fig. 1(d), the BSBCz:CBP layers both with and without the  $\text{TeO}_x$  layer show high PLQYs ( $>90\%$ ), indicating that the deposition of  $\text{TeO}_x$  has a negligible influence on the organic layer beneath. In contrast, Rajendran *et al.*<sup>19</sup> had reported a top DBR fabricated by a sputtering method, where the PLQY of the organic layer dropped significantly from  $\sim 90\%$  to 34%. It is also reported that by inserting a protective layer such as  $\text{LiF}$ <sup>2</sup> or poly(methyl methacrylate) (PMMA),<sup>31</sup> it is possible to maintain a high PLQY; however, the insulating protective layer prevents the device from being useful for current injection. To make a better comparison, we also examined the BSBCz:CBP layer covered by a room temperature e-beam evaporated  $\text{TiO}_2$  film (60 nm).  $\text{TiO}_2$  films both without ( $\text{TiO}_2$ -a) and with ( $\text{TiO}_2$ -b) an end-Hall ion source were prepared. As shown in Fig. 1(d), for the  $\text{TiO}_2$ -a sample, the PLQY severely drops to around 13%, which evidently demonstrates the damage of the e-beam process. The  $\text{TiO}_2$ -b sample exhibits an even lower PLQY ( $\sim 11\%$ ). These results clearly show that the thermally evaporated top DBR in this work is highly compatible with organic gain materials.

Figure S4(a) presents the transmittance of a 7.5 pair top DBR. It has a stop band from 440 nm to 530 nm, which well covers the PL of BSBCz:CBP. The measured transmittance agrees well with the calculated one using the transfer matrix method<sup>32</sup> and shows a high reflectance ( $\sim 99.4\%$ ) within the stop band. Increasing the stack from 7.5 pairs to 10.5 pairs leads to a higher reflectance of  $\sim 99.8\%$  [Fig. S4(b)]. One can expect even higher reflectance by further increasing the

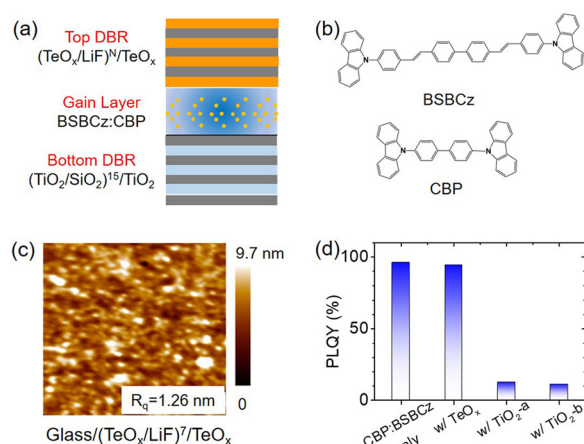


**FIG. 1.** (a) Schematic of the OVCSEL, (b) molecular structures of the gain material, (c) atomic force microscope images for  $\text{TeO}_x$ -ended 7.5 pairs of the top DBR, and (d) PLQY for BSBCz:CBP films with different capping layers.

number of pairs, which are useful in improving the optical confinement and lowering the optical loss of OVCSELs.<sup>33</sup>

Figure 2 presents the lasing characteristics of the devices with 7.5 pair and 10.5 pair top DBRs. At first, the devices were pumped by a short-pulsed (0.8 ns) nitrogen laser. For the device with the 7.5-pair top DBR, a weak spontaneous emission centered at 458.7 nm could be observed at a low pump fluence [Fig. 2(a)]. As the pump fluence increases, a narrow emission spectrum appears at 460.0 nm, which characterizes the advent of lasing. The emission intensity and full width at half maximum (FWHM) linewidth of the lasing mode as a function of pump fluence are shown in Fig. 2(b). It suggests a clear threshold of  $\sim 5.5 \mu\text{Jcm}^{-2}$  as confirmed by the sudden change of the intensity slope and the sharply narrowed linewidth (0.29 nm). The inset of Fig. 2(b) shows the log-log plot of the emission intensity, where a typical S-shape curve could be found, from which the spontaneous emission factor  $\beta$  with a value of  $\sim 0.04$  can be estimated.<sup>34,35</sup> This value is fairly large compared with typical values ( $10^{-4} \sim 10^{-3}$ ) in the literature,<sup>12,31,36</sup> which is favorable for reducing device threshold.<sup>37</sup> This large value of  $\beta$  can be attributed to the short cavity since  $\beta$  is inversely proportional to the cavity length.<sup>34</sup>

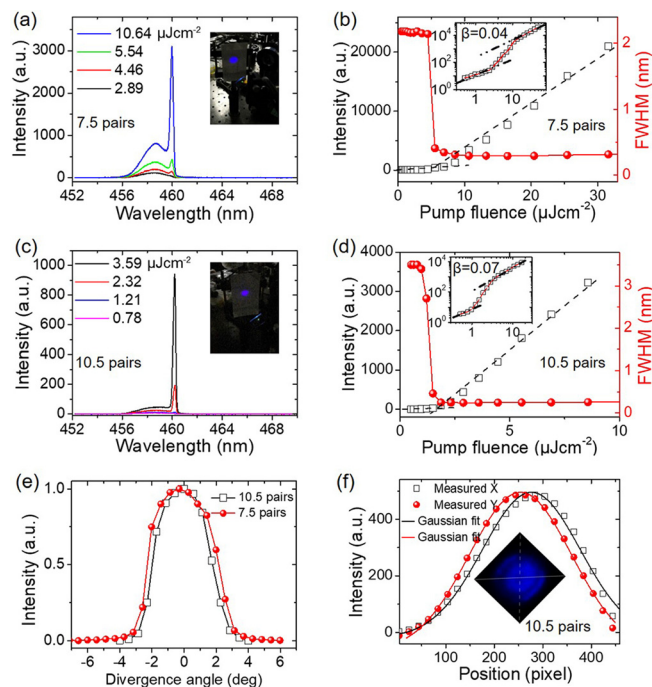
For excitation above the threshold, we can clearly observe a far field circular spot on a paper screen placed 10 cm away from the device [inset of Fig. 2(a)]. The diameter of the spot is  $\sim 10$  mm, indicating a divergence angle of less than  $3^\circ$  [Fig. 2(e)], which is among the best

results for microcavity devices ever reported (Table S1). We can estimate the beam quality factor ( $M^2$ ) to be of the order of  $M^2 \sim \pi w \theta_{1/2} / \lambda = 20$ , where  $w$  is the beam radius onto the OVCSEL ( $\sim 150 \mu\text{m}$ ) and  $\theta_{1/2}$  is the far-field angular half-width at half maximum ( $\sim 2.2^\circ$ ). This value is higher than an ideal diffraction-limited beam having  $M^2 = 1$ , which could be attributed to multi-transverse modes under large area pumping. As will be shown later, the value can be dramatically reduced by using a pump beam with a smaller area. We also recorded the far field pattern [inset of Fig. 2(f)], whose intensity profile can be well fitted by the Gaussian function in both x and y directions (Table S2).

It is well known that a high quality (Q) factor enables a low lasing threshold as a result of the reduced optical loss and improved spontaneous emission factor.<sup>37–39</sup> The FWHM linewidth for the device with a 10.5 pair top DBR shows a narrower value of 0.24 nm [Fig. 2(d)] compared to that for the device with a 7.5 pair top DBR. Although the laser linewidth does not enable a direct measurement of the Q-factor, the reduced linewidth and, most importantly, the reduced threshold indicate an improved Q-factor upon increasing the pairs of the top DBR. Indeed, a single longitudinal mode lasing occurs at 460.2 nm [Fig. 2(c)], which is very close to that for the device with a 7.5 pair top DBR, however, with much lower threshold of only  $1.7 \mu\text{Jcm}^{-2}$  [Fig. 2(d)]. The log-log plot [inset of Fig. 2(d)] of the emission intensity also shows a clear S-shape curve, suggesting an improved  $\beta$  of  $\sim 0.07$ . The reduction of the threshold is consistent with the improved Q-factor and  $\beta$ . This threshold is not only orders of magnitude lower among the OVCSELs with non-destructive top DBRs but also comparable with other reported high performance planar microcavity devices (Table S1). It should be noted that the incorporation of different gain materials from the literature can also lead to the low threshold, which, however, is beyond the scope of the current work. The device with a 10.5 pair top DBR also shows a good directionality with a divergence angle even smaller than that for the device with a 7.5 pair top DBR [Fig. 2(e)].

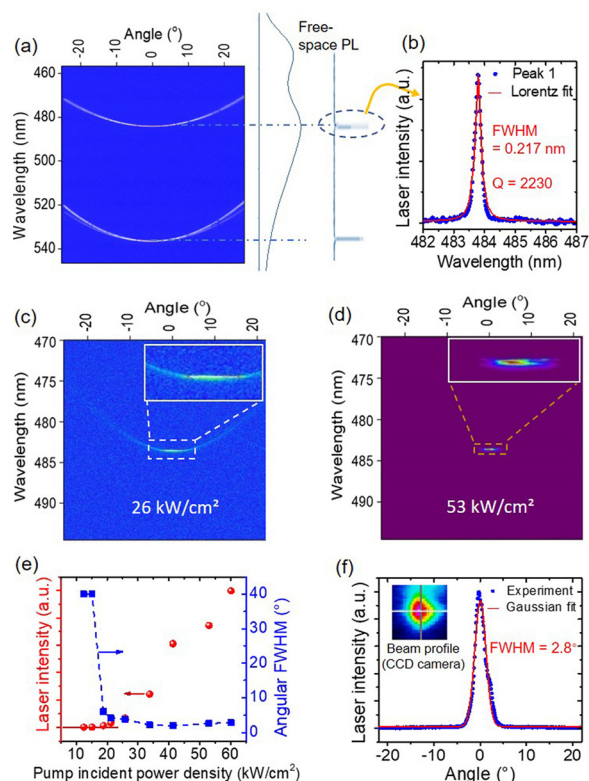
Encouraged by the low threshold under sub-ns short pulse pumping, we further investigated the lasing performance of the device with the 10.5 pair top DBR mirror under diode pumping, which represents an important step toward the elaboration of very compact devices at low cost that can be more directly transferrable for applications. As diode laser pulses used for organic microcavity laser pumping have usually pulse widths that are longer than the radiative lifetime (a few ns or longer), diode-pumping experiments also enable testing the ability of materials to work in the long-pulse regime, which is important in the quest for continuous-wave (CW) lasing. In order to fully characterize both spatial and spectral lasing properties, we used here a Fourier-plane imaging system (Fig. S5) to collect the angle-resolved emission spectrum. Unlike the nitrogen laser excitation at 337 nm, excitons are generated on BSBCz molecules directly when excited under 405 nm and do not result from a Förster energy transfer from the host due to the weak negligible absorption of CBP at 405 nm (Fig. S6). Therefore, we increased the film thickness to 600 nm to guarantee effective absorption while maintaining a low doping concentration of BSBCz to keep a high value of the PLQY.

Figure 3(a) shows the angle-resolved PL spectrum for the device. As a result of increased thickness, two emission modes centered at 483.8 nm and 536.8 nm emerge. Both modes show the characteristic parabolic dispersion as the viewing angle increases. The mode at



**FIG. 2.** Lasing characteristics of OVCSELs: panels (a) and (b) and panels (c) and (d) are emission spectra, emission intensity, and FWHM linewidth under different pump fluences for the device with a 7.5 pair top DBR and with a 10.5 pair top DBR, respectively. Insets of panels (a) and (c) and panels (b) and (d) are the far field pattern and the emission intensity in the log-log plot, respectively. (e) Divergence angle of the OVCSELs. (f) Far field pattern for the device with a 10.5 pair top DBR and the Gaussian fit for the intensity profiles in two perpendicular directions.





**FIG. 3.** (a) Angular and spectral PL colormap recorded below the threshold for the OVCSEL capped with the 10.5-pair DBR top mirror. Two resonant peaks with parabolic dispersion are visible inside the PL bandwidth in free space (shown on the right). (b) Zoom on the 483.8 nm peak superimposed with a Lorentzian fit. (c) and (d) Evolution of the parabolic map of (a) over lasing threshold. (e) Laser intensity (left) and angular FWHM (right) vs pump power density. (f) Spectrally integrated laser emission @ 60 kW/cm<sup>2</sup> vs angle. Inset: beam profile at a distance of ~30 cm from the device.

483.8 nm is well located within the high gain spectrum range of BSBCz:CBP and is the only mode to show lasing. A Lorentz fit of this mode (below lasing threshold emission at 0°) gives a Q-factor for the passive cavity as high as 2230 [Fig. 3(b)]. This high Q-factor is partly explained here by the longer cavity.

Figures 3(c)–3(f) show lasing properties of the device. In Figs. 3(c) and 3(d), two spectral Fourier images show how the characteristic parabolic dispersion of PL, still visible near threshold, becomes concentrated around normal incidence to give birth to a single bright spot, indicating the concentration of emission both in the spectrum and in the angle, which is evidence of photon lasing in a weak coupling regime. As the pump duration is much longer than radiative lifetime, threshold is now reported in units of pump power density<sup>32</sup> and is about 18 kW/cm<sup>2</sup> [Fig. 3(e)]. Very few studies have reported the thresholds under long-pulse pumping for OVCSELs,<sup>28,40</sup> but threshold has a comparable order of magnitude<sup>31,40</sup> or is even smaller than those of some reports.<sup>22,28</sup> As shown in Fig. 3(e), the angular linewidth shows dramatic narrowing after threshold, a value that is in accordance with previous results under sub-ns pumping. From the far-field divergence (~2.8°) and beam radius (~16 μm) on the sample, we can

also estimate the  $M^2$  to be of the order of 2.5, which is now comparable with that of an ideal diffraction-limited beam having  $M^2 = 1$ , indicating a very good beam quality for the OVCSEL, comparable to those reported in inorganic low-power VCSELs<sup>41</sup> with in addition a beam showing good circularity as shown in Fig. 3(f) (inset).

In summary, we have demonstrated that thermal evaporation is an attractive technique to fabricate high quality top DBR mirrors for OVCSELs. The OVCSEL realized in this work shows a low threshold (1.7 μJ/cm<sup>2</sup> under nitrogen laser pulsed pumping and 18 kW/cm<sup>2</sup> under long-pulse diode-pumping), low angular divergence < 3°, and good beam quality ( $M^2 = 2.5$ ). This highlights the merits of this non-destructive and high process-tolerant technique. Our results may open a promising route for future high performance microcavity optoelectronic devices, especially for laser devices based on soft materials.

See the [supplementary material](#) for the details of the experiments, optical properties, and morphology for the films and devices; summary of device performance in the literature; Gaussian fitting of the far field pattern; and Fourier-imaging setup.

This work was funded by the National Natural Science Foundation of China under Nos. 61875195, 61975256, and 51973208, Jilin Province Science and Technology Research Project No. 20190302087GX, the Japan Science and Technology Agency (JST), ERATO, the Adachi Molecular Exciton Engineering Project (JST ERATO Grant No. JPMJER1305), and by the International Institute for Carbon-Neutral Energy Research (No. WPI-I2CNER).

## DATA AVAILABILITY

The data that support the findings of this study are available from the corresponding author upon reasonable request.

## REFERENCES

- <sup>1</sup>S. Chenais and S. Forget, *Polym. Int.* **61**, 390 (2012).
- <sup>2</sup>A. J. C. Kuehne and M. C. Gather, *Chem. Rev.* **116**, 12823 (2016).
- <sup>3</sup>I. D. W. Samuel and G. A. Turnbull, *Chem. Rev.* **107**, 1272 (2007).
- <sup>4</sup>C. Karnutsch, C. Plumm, G. Heliotis, J. C. Demello, D. D. C. Bradley, J. Wang, T. Weimann, V. Haug, C. Gartner, and U. Lemmer, *Appl. Phys. Lett.* **90**, 131104 (2007).
- <sup>5</sup>Y. Yang, G. A. Turnbull, and I. D. W. Samuel, *Appl. Phys. Lett.* **92**, 163306 (2008).
- <sup>6</sup>A. S. D. Sandanayaka, T. Matsushima, F. Bencheikh, K. Yoshida, M. Inoue, T. Fujihara, K. Goushi, J. C. Ribierre, and C. Adachi, *Sci. Adv.* **3**, e1602570 (2017).
- <sup>7</sup>Y. Jiang, P. Lv, J. Q. Pan, Y. Li, H. Lin, X. W. Zhang, J. Wang, Y. Y. Liu, Q. Wei, G. C. Xing, W. Y. Lai, and W. Huang, *Adv. Funct. Mater.* **29**, 1806719 (2019).
- <sup>8</sup>Q. Zhang, J. G. Liu, Q. Wei, X. R. Guo, Y. Xu, R. D. Xia, L. H. Xie, Y. Qian, C. Sun, L. Luer, J. Cabanillas-Gonzalez, D. D. C. Bradley, and W. Huang, *Adv. Funct. Mater.* **28**, 1705824 (2018).
- <sup>9</sup>E. B. Namdas, M. Tong, P. Ledochowitsch, S. R. Mednick, J. D. Yuen, D. Moses, and A. J. Heeger, *Adv. Mater.* **21**, 799 (2009).
- <sup>10</sup>N. Tessler, G. J. Denton, and R. H. Friend, *Nature* **382**, 695 (1996).
- <sup>11</sup>M. Koschorreck, R. Gehlhaar, V. G. Lyssenko, M. Swoboda, M. Hoffmann, and K. Leo, *Appl. Phys. Lett.* **87**, 181108 (2005).
- <sup>12</sup>M. C. Gather and S. H. Yun, *Nat. Commun.* **5**, 5722 (2014).
- <sup>13</sup>J. Lin, Y. Hu, Y. Lv, X. Guo, and X. Liu, *Sci. Bull.* **62**, 1637 (2017).
- <sup>14</sup>M. T. Hill and M. C. Gather, *Nat. Photonics* **8**, 908 (2014).
- <sup>15</sup>O. Mhibik, S. Forget, D. Ott, G. Venus, I. Divliansky, L. Glebov, and S. Chénais, *Light: Sci. Appl.* **5**, e16026 (2016).

- <sup>16</sup>A. S. D. Sandanayaka, T. Matsushima, F. Bencheikh, S. Terakawa, W. J. Potscavage, C. J. Qin, T. Fujihara, K. Goushi, J. C. Ribierre, and C. Adachi, *Appl. Phys. Express* **12**, 061010 (2019).
- <sup>17</sup>L. Persano, A. Camposeo, P. Del Carro, E. Mele, R. Cingolani, and D. Pisignano, *Opt. Express* **14**, 1951 (2006).
- <sup>18</sup>M. S. Alias, Z. X. Liu, A. Al-atawi, T. K. Ng, T. Wu, and B. S. Ooi, *Opt. Lett.* **42**, 3618 (2017).
- <sup>19</sup>S. K. Rajendran, M. J. Wei, H. Ohadi, A. Ruseckas, G. A. Turnbull, and I. D. W. Samuel, *Adv. Opt. Mater.* **7**, 1801791 (2019).
- <sup>20</sup>L. Persano, P. Del Carro, E. Mele, R. Cingolani, D. Pisignano, M. Zavelani-Rossi, S. Longhi, and G. Lanzani, *Appl. Phys. Lett.* **88**, 121110 (2006).
- <sup>21</sup>N. Pourdavoud, T. Haeger, A. Mayer, P. J. Cegielski, A. L. Giesecke, R. Heiderhoff, S. Olthof, S. Zaefferer, I. Shutsko, A. Henkel, D. Becker-Koch, M. Stein, M. Cehovski, O. Charfi, H. H. Johannes, D. Rogalla, M. C. Lemme, M. Koch, Y. Vaynzof, K. Meerholz, W. Kowalsky, H. C. Scheer, P. Gorn, and T. Riedl, *Adv. Mater.* **31**, e1903717 (2019).
- <sup>22</sup>Y. Wang, X. M. Li, V. Nalla, H. B. Zeng, and H. D. Sun, *Adv. Funct. Mater.* **27**, 1605088 (2017).
- <sup>23</sup>C. Y. Huang, C. Zou, C. Y. Mao, K. L. Corp, Y. C. Yao, Y. J. Lee, C. W. Schlenker, A. K. Y. Jen, and L. Y. Lin, *ACS Photonics* **4**, 2281 (2017).
- <sup>24</sup>M. Anni, G. Gigli, R. Cingolani, S. Patane, A. Arena, and M. Allegrini, *Appl. Phys. Lett.* **79**, 1381 (2001).
- <sup>25</sup>M. Muallem, A. Palatnik, G. D. Nessim, and Y. R. Tischler, *ACS Appl. Mater. Interfaces* **7**, 474 (2015).
- <sup>26</sup>P. G. Savvidis, L. G. Connolly, M. S. Skolnick, D. G. Lidzey, and J. J. Baumberg, *Phys. Rev. B* **74**, 113312 (2006).
- <sup>27</sup>G. Canazza, F. Scotognella, G. Lanzani, S. De Silvestri, M. Zavelani-Rossi, and D. Comoretto, *Laser Phys. Lett.* **11**, 035804 (2014).
- <sup>28</sup>L. M. Goldenberg, V. Lisinetskii, and S. Schrader, *Laser Phys. Lett.* **10**, 055808 (2013).
- <sup>29</sup>Y. Hu, J. Lin, L. Song, Q. Lu, W. Zhu, and X. Liu, *Sci. Rep.* **6**, 23210 (2016).
- <sup>30</sup>B. Deveaud, *The Physics of Semiconductor Microcavities* (Wiley-VCH, 2007), pp. 31–43.
- <sup>31</sup>S. T. Chen, C. Zhang, J. Lee, J. Han, and A. Nurmikko, *Adv. Mater.* **29**, 1604781 (2017).
- <sup>32</sup>S. Forget and S. Chenais, *Organic Solid-State Lasers* (Springer, 2013), pp. 68–69.
- <sup>33</sup>L. Persano, A. Camposeo, P. Del Carro, E. Mele, R. Cingolani, and D. Pisignano, *Appl. Phys. Lett.* **89**, 121111 (2006).
- <sup>34</sup>S. Morimura and K. Ujihara, *Jpn. J. Appl. Phys., Part 1* **36**, 4307 (1997).
- <sup>35</sup>R. Brueckner, M. Sudzius, H. Froeb, V. G. Lyssenko, and K. Leo, *J. Appl. Phys.* **109**, 103116 (2011).
- <sup>36</sup>M. Sudzius, M. Langner, S. I. Hintschich, V. G. Lyssenko, H. Froeb, and K. Leo, *Appl. Phys. Lett.* **94**, 061102 (2009).
- <sup>37</sup>H. Yokoyama, *Science* **256**, 66 (1992).
- <sup>38</sup>G. Bjork and Y. Yamamoto, *IEEE J. Quantum Electron.* **27**, 2386 (1991).
- <sup>39</sup>H. Zhu, Y. Fu, F. Meng, X. Wu, Z. Gong, Q. Ding, M. V. Gustafsson, M. T. Trinh, S. Jin, and X. Y. Zhu, *Nat. Mater.* **14**, 636 (2015).
- <sup>40</sup>H. Sakata and H. Takeuchi, *Appl. Phys. Lett.* **92**, 113310 (2008).
- <sup>41</sup>J. Blane, W. North, P. Zeidler, J. Dencker, D. Chacko, B. Souhan, K. Ingold, and J. Raftery, *Proc. SPIE* **9766**, 97660I (2016).